



## A NEW MASS LESION IDENTIFICATION USING CONVOLUTIONAL NEURAL NETWORKS IN MAMMOGRAPHY

<sup>1</sup>Md Altab Uddin Molla, <sup>2</sup>Souradeep Sarkar, <sup>3</sup>Chandan Ghosh, <sup>4</sup>Nitu Saha

<sup>1</sup>Assistant Professor, <sup>2</sup> Assistant Professor, <sup>3</sup> Assistant Professor, <sup>4</sup> Assistant Professor

<sup>1</sup>Computational Science Department,

<sup>1</sup>Brainware University, Kolkata, India

**Abstract:** When using learning-based approaches, mammography image analysis, feature extraction is a critical step. Traditionally, the content of images is represented by handcrafted, problem-dependent features. Neural networks are a different strategy that has been successfully used in other fields to automatically find good features. Learning the characteristics of mammography mass tumors and then feed those features to a classification step, convolutional neural networks are evaluated in this work. The results of the research verified that this strategy is effective, in terms of the area under the ROC curve, it outperformed the most recent representation by 79.9% to 89%.

**Index Terms - Breast cancer, Duplicate descriptors, Histogram of oriented gradients (HOG), Mammography classifiers**

### I. INTRODUCTION

Breast tumor is the maximum prevalent type of tumor in the female society worldwide, through over 1.5 million expected identifies in 2010 and additional 500,000 deaths annually [1]. Because mammography can detect breast cancer during its recognized asymptomatic period, it serves as the major imaging technique for testing. Double reading, performed by two radiologists reading the similar mammograms separately has been recommended to decrease the percentage of wasted malignancies and is presently a part of the majority of broadcast programme [2]. However, results in more labor and expenses. As an alternative, computer-aided diagnosis (CADx) tools can supplement the judgments of a single radiologist reading mammograms. These systems are designed to categories lesions found by the radiologist.

Machine learning classifiers (MLC) are usually used by CADx systems to offer judgement. A set of structures defining the picture is needed in command to train an MLC for breast cancer analysis. High discriminant power features are those that can tell if a particular the image comes from a tumor finding. However, because it is a difficult subject, researchers from a variety of disciplines—from medicine to computer vision—have turned their attention to it. As a result, the diagnosis might be inferred from a variety of features. In many CADx systems, features are manually created based on prior knowledge and professional advice. Deep learning is the name of this paradigm.

Recently, several computer perception tasks have been addressed using deep learning techniques [3]. Their biggest benefit comes from eschewing the creation of specialized feature detectors. Deep learning models, on the other hand, automatically learn representative characteristics from the data. Particularly when it comes to computer vision issues like object detection and natural scene classification, deep learning has produced impressive results [3]. Deep learning prototypes have been applied to a variation of curative tasks, including segmenting sclerosis lesions, diagnosing Alzheimer's disease, and classifying tissues in histology and histopathology pictures [4–5].

Only a small number of studies, however, have investigated deep learning techniques to handle the task of automatically analyzing mammogram images [1]. Convolutional neural network (CNN) models with multiscale features are presented in [6]. were utilized to segregate breast tissue and estimate breast density score using stacked deep auto-encoders. In [7], CNNs are employed as a representation approach to describe micro calcifications. The closest study that used an adaptive deconvolutional network to learn the representation needed to distinguish between malignant and benign breast tumours is [8]. In contrast, this research offers an assessment of convolutional architectures for learning the representation of images. Given that we employ supervised data while training CNN, its key distinction from earlier efforts relates to how features are learned. This strategy makes use of the lesion annotation, which was manually created by skilled radiologists, which contains expert understanding.

The rest of the essay is controlled as follows: The suggested method for doing automatic mammography picture analysis is described in Section II. The experimental setup utilized to assess the suggested technique is described in Section III. Sections IV and V reveal the results and explain the key findings of this effort to conclude.

## II. COMPACTED AS WELL AS APPROACHES

### Breast tumor numerical depository

The benchmarking dataset used in this investigation may be found in the breast cancer digital repository (BCDR)2. The Breast Cancer Data Resource (BCDR) is a substantial, annotated public repository that contains the cases of breast cancer patients from Pakistan's northern area. In addition to presenting typical and highlighted breast cancer patient cases, BCDR also offers pre-computed image-based descriptors, radiologists' observations of anomalies, and outlines of mammography lesions and other related clinical data. A brand-new "Film Mammography-based dataset" was utilized in this study (BCDR-F03). The BCDR-F03, which was taken directly from the BCDR, consists of 456 individuals with 856 film images of 536 benign and 410 malignant mass lesions, together with clinical information and picture-based descriptors. Figure 1 displays instances of benign and malignant lesions together with their corresponding segmentations.

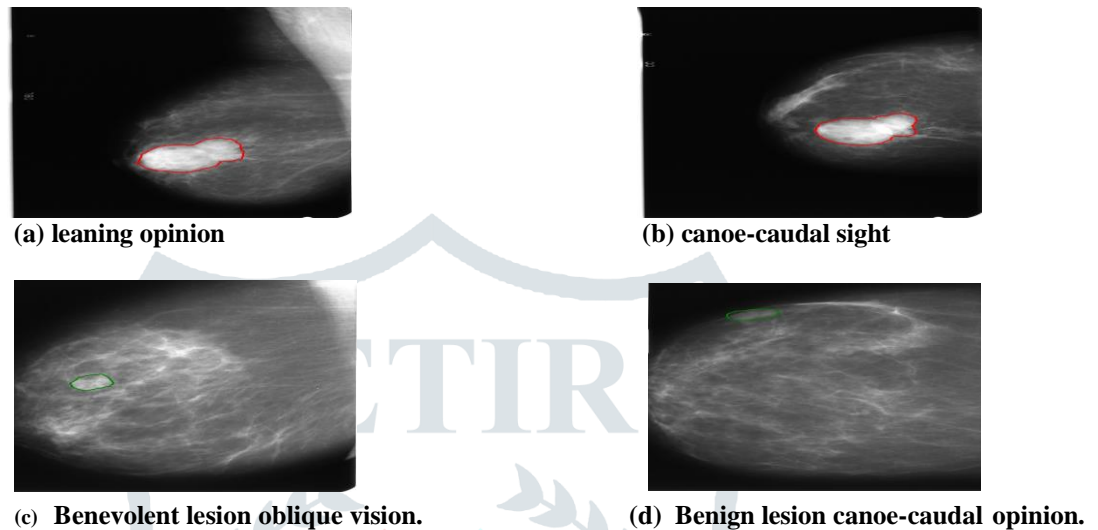


Fig. 1: Examples of the dataset's photos.

Category	Structures
Strengths	Highest, lowest, skewness, kurtosis, standard deviation, mean
Figure	Area, border, obliqueness, elongation, y_center_tumor, x_center_tumor,
Surfaces	Gap, connection

TABLE I: Handcrafted topographies set. For facts [3]

- Basic descriptor:** The histogram of gradients (HOG) descriptor and histogram of gradient divergence (HGD) were chosen as our starting point then they performed the maximum when compared to other conventional descriptors, according to the systematic evaluation published by [2]. In addition, a collection of 17 manually created features relating to the surface and strengths of the images are used for comparison. These features were recovered from segmented lesions.
  - Handmade characteristics (HC):** A double-step technique was recycled to choose the handcrafted features: (1) the Perez et al. [9] feature selection method was applied to the original set of features [2] in order to rank the features; and (2) a set of 17 texture, shape, and intensity features with high performance to describe masses were heuristically chosen. Features are categorized in Table I based on their type. It is made up of shape descriptors calculated from the radiologists' determined lesion's contour, texture descriptors derived from the radiologists' determined lesion's bounding box, and intensity descriptors computed directly from the radiologists' determined lesion's grey-levels of the pixels inside the lesion's contour. Keep in mind that this set of features necessitates not only the expert's manual segmentation but also the region of interest (ROI) detection.
  - Histogram of oriented gradients (HOG):** It uses the ramp's spreading to describe picture. A histogram of the gradient's direction is used to characterize each block in a grid of blocks made up of images (such as 3 3). Each histogram has a predetermined number of bins that divide the range of potential orientations (from 0 to 2 radians, or from 0 to radians), and each bin's value is determined by adding the gradient amplitudes of all the pixels that fall inside the bin's boundaries.
  - Histogram of gradient divergence (HGD):** Gradient divergence in a point(  $i, j$  ) is determined by measuring the angle between a vector travelling toward the center of the picture with its origin at a point (  $i, j$  ) and a vector representing the

intensity gradient on  $x(i, j)$ . Images are referred to in HGD as the gradient divergence distribution [2]. Each zone in the image is defined by a histogram of the gradient divergence. Images are segmented into concentric sections.

### III. SUGGESTED TECHNIQUE

Image representation is essential for mammography image analysis that is automated. Its objective is to provide a concise and discriminating description of the image's content. In order to define the lesion, CADx systems that are commonly used for mammography computer vision express images with a well-chosen set of mathematical and experiential properties. A learning-based solution has recently been developed to replace this manual engineering process [8], [6]. This method transforms the unprocessed pixels in a regular of characteristics that feed a classifier process into a model in an unsupervised way. As opposed to earlier research, we used a hybrid strategy here, where CNNs are utilized to learn the representation in administered manner. In other words, we directed the feature learning process using the annotations.

Pretreatment, image compression, and arrangement training are the three key phases of our methodology. The goal of preprocessing, which is described in sector II-B.1, is to get the data ready using a variety of transformations so that the subsequent stage can benefit from pertinent qualities. A CNN is trained using annotated examples to accomplish feature learning, which is covered in sector II-B.2. The final step, described in sector II-B.3, the process of a CNN's penultimate layer's properties being used to train an SVM classifier.

**Pretreatment:** In CADx systems, preprocessing is a typical stage. By using a set of adjustments that could aid to increase performance in subsequent phases, its main objective is to improve the image's attributes. The ROI must be extracted from the image as the initial stage in this project. Second, a technique known as oversampling is utilized to both generate extra samples and aid in avoiding overfitting during training. The data is then normalized in order to get it ready for learning processes. These actions are described below:

- **Image compression:** For accessibility, we set the input size to  $(r \times r)$  pixels (e.g. 200x200). When appropriate, images were rescaled to  $(r \times r)$  pixels and reaped to the hopping box of the segmented lesion; otherwise, the surrounding area was maintained. This was done because the BCDR dataset offers manual segmentation.
- **Data bionic implants:** We have affectedly created 9 novel label-preserving tasters for each training image by combining sealing and rotation transformations of 90, 180, 270 and 360 degrees. A lesion can be presented in any direction; therefore data augmentation makes sense for the lesion classification problem. The model should therefore be able to pick up new information from these modifications.
- **Quantization:** During the digitalization process, different film images' lighting conditions would have varying effects on all of the image's pixel values. To combat this effect, people frequently use a global contrast. During normalization, each pixel is subtracted from the average of the image's intensities. Additionally, local contrast normalization (LCN) was carried out. By doing normalization in tiny areas throughout the entire image, its major goal is to imitate the behavior of the V1 visual cortex [10]. It is well known that decorrelated and normalized input data generally improve the performance of feature culture and deep knowledge methods, primarily because these properties promote the convergence of gradient-based optimization strategies [10]. It should be noted that both worldwide and gap stabilizations are carried out image-wise, negating the need to save parameters during the training process.

**Supervised feature culture:** Using connections exchanged between hidden units, CNN, a multilayer perceptron, provides rapid calculation speeds and features of translational invariances. CNNs have been used effectively. as shining in medical analyses where texture served as a discriminant characteristic [4], circumstances involving form identification [11]. A CNN model provides an effective method for classifying mass lesions since mass representation is substantially associated with form and texture variables [1], [2].

- **Architecture:** The activation function, pooling function, and convolutional kernels are the three essential components of a CNN layer. A collection of several tiny squares known as a convolutional kernel acts as a filter on the input picture. The output of this effort is the activation function's input, which contains element-wise non-linearity's. Finally, the pooling function uses an aggregating function like max to combine contiguous values (). These three elements are iteratively built on top of one another to escalation the model's volume, resulting in the creation of a deep neural network that has two layers or more.



Fig. 2: Finest CNN estimated on mass arrangement

The suggested architecture, shown in figure 2, starts with 12 x12 limited kernels in the first layer and then transitions to a 6x 6 pooling structure with a 2x 2-pixel stride. The second layer has 6x 6 local kernels that don't overlap and have a 2x2 pooling structure. The third fully linked layer has a maximum of 500 units.

- Learning algorithm:** Usually, classifier models with many parameters overfit training data, making it difficult for them to generalize to untrained data. Different tactics are needed to manage this tendency in neural networks, which is not an exception. Dropout and max-norm regularization were employed in this study. In contrast to dropout [12], which randomly sets a unit's input to 0. max-norm regularization drives each vector of incoming weights in a unit to have its norm set to a maximum value.
- Optimization:** In our using technique cutting the structure based on CNN in mass arrangement. The validation set's part below the ROC curve (AUC) was used as the stop criterion for an early stopping method. The Pylearn2 framework, which effectively and heavily utilizes GPU processing resources, was used to implement the suggested method [13]. The infrastructure of the CETA-CIEMAT2 Research Center was used for a substantial investigation. A NVidia Tesla K40 GPGPU card was used to run larger models that needed more demanding computing.

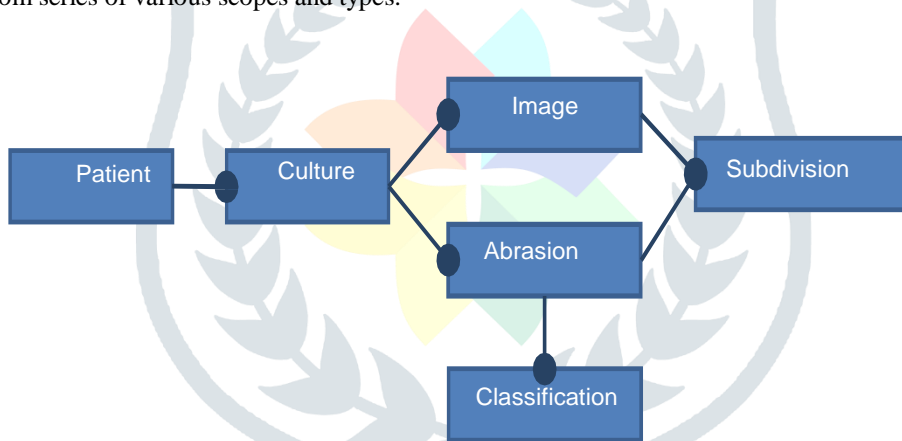
**Classification:** Linear SVM was used as the classification approach in accordance with earlier research [8], [2]. Up until the last layer, image areas are relayed across the network, and their activations are employed as a representation to assess CNN as a representation technique. In this stage, a smaller model is changed as part of the final layer's fine-tuning procedure.

#### IV. EXPERIMENTAL OPERATION

Following stratified patient sampling, the unique BCDR-F03 dataset was split into working out (60%) and particle dataset (40%), with each patient's mammograms being assigned to just one of the two subsets. This configuration ensures that the model is not evaluated during the training stage using actual patients.

Depending on how the lesions are distributed and computing power, the cropped region's size was set during the preprocessing stage to  $r = 210$ , and for LCN,  $k = 20$  pixels was chosen as the kernel scope. Block sizes for HOG and HGD are 6 by 6 and 2 by 2, respectively, it was investigated in accordance with prior findings [2]. Both histograms were examined using 4 and Sixteen bins.

Before supplying data to any MLC, a dataset must be normalized because distinct properties shared by all vectors typically earnings values from series of various scopes and types.



25 models were trained with random hyperparameter initialization using the validation set is one-sixth of the training set, and the top model was chosen based on validation performance. When training deep models, it is claimed that this approach is better than grid search [14]. A zero-mean unit-variance normalization technique is used before training the SVM model. 20 bootstrap runs without replacement on the SVM classifier's, C parameter was changed using the training set. Ending performance is represented by the test set's area under the ROC curve (AUC).

#### V. RESULTS

A summary of these investigations is shown in Table II. The segmentation-based HCfeats set outperforms HOG-based descriptors by a small margin. This demonstrates how crucial shape data is for mass characterization. It's interesting to note that CNN models that merely use raw pixels,

	Cultured			Starting point		
<b>Structures</b>	<b>CNN<sub>3</sub></b>	De-CAF	CNN5	HOG2	HGD3	HC
<b>AUC1</b>	<b>0.860</b>	0.836	0.821	0.796	0.793	0.799

<b>AUC2</b>	<b>0.96</b>	0.90	0.860	0.852	0.843	0.830
-------------	-------------	------	-------	-------	-------	-------

**TABLE II: Results summary for the test set in terms of AUC.**

surpass the performance of cutting-edge features [2]. It is also noteworthy that increasing the number of layers in the model enhances its capacity for representation, producing the finest outcomes.

For comparison's sake, we evaluated DeCAF [15], a pretrained model, using the Imagenet dataset 3. DeCAF is more advanced than any other evaluated representations and other models. As a result, it is anticipated to perform better than features that are handcrafted. The best performance comes from a smaller CNN model that was trained using photos from the domain. This conduct supports the following two findings: On the one hand, for autonomous mammography picture analysis, CNN models outperform cutting-edge representations. In order to teach the model the textural and form features present in mass lesions, the learning process should be guided by a training set with a wide range of visual variability. A large CNN model, however, is not enough to learn the representation since some properties are problematic for automatic analysis.

## VI. CONCLUSIONS

In this work, a system for categorizing mass lesions in mammography film images is proposed. It may be concluded that instead of inventing specific characteristics to describe the content of mammography images, this method directly learns the features from data in a supervised manner. The suggested CNN architecture learns a set of nonlinear transformations from the input pixels of the picture in order to better precisely represent the image data. In terms of the area below the ROC curve, our method fared better than cutting-edge techniques, HOG and HGD identifiers [21], by 79.9% to 89.0%. (AUC). It's noteworthy that this model outperforms a set of manually constructed features as well, taking improvement of the extra knowledge. Our upcoming study will evaluate larger designs and incorporate clinical data in an effort to improve representation.

## VII. ACKNOWLEDGEMENTS

The "Mais Centro" initiative of QREN and the Cloud Thoughtful plan (CENTRO-07-ST24-FEDER-002031) provided the primary funding for this effort (Portugal). Additionally, it received some funding from the European Regional Development Fund's "Diseo y implementación de un sistema de cómputo sobre recursos heterogéneos para la identificación de estructuras atmosféricas en predicción climatológica" project, as well as from the computing resources of the Extremad (ERDF)[26]. Spanish government Arevalo also expresses gratitude to Colciencias for its assistance with a PhD grant under call 617/2013. The K40 Tesla GPU from NVIDIA, which was provided as a gift and used for various feature learning studies, is also acknowledged by the authors.

## REFERENCES

- [1] D. C. Moura and M. A. Guevara López, "An evaluation of image descriptors combined with clinical data for breast cancer diagnosis," *International Journal of Computer Assisted Radiology and Surgery*, vol. 8, no. 4, pp. 561–574, 2013.
- [2] Y. Bengio, A. Courville, and P. Vincent, "Representation learning: A review and new perspectives," *Pattern Analysis and Machine Intelligence*, *IEEE Transactions on*, vol. 35, pp. 1798–1828, Aug 2013.
- [3] J. Arevalo, A. Cruz-Roa, and F. A. González, "Hybrid image representation learning model with invariant features for basal cell carcinoma detection," 2013.
- [4] G. Wu, D. Zhang, and L. Zhou, eds., *Machine Learning in Medical Imaging*. Springer International Publishing, 2014.
- [5] K. Petersen, M. Nielsen, P. Diao, N. Karssemeijer, and M. Lillholm, "Breast Tissue Segmentation and Mammographic Risk Scoring Using Deep Learning," in *Breast Imaging* (H. Fujita, T. Hara, and C. Muramatsu, eds.), vol. 8539 of *Lecture Notes in Computer Science*, pp. 88–94, Springer International Publishing, 2014.
- [6] X.-S. Zhang, "A new approach for clustered MCs classification with sparse features learning and TWSVM.," *The Scientific World Journal*, vol. 2014, p. 970287, Jan. 2014.
- [7] A. R. Jamieson, K. Drukker, and M. L. Giger, "Breast image feature learning with adaptive deconvolutional networks," 2012.
- [8] N. P. Pérez, M. A. G. López, A. Silva, and I. Ramos, "Improving the mann-whitney statistical test for feature selection: An approach in breast cancer diagnosis on mammography," *Artificial Intelligence in Medicine*, no. 0, pp. –, 2014.
- [9] K. Jarrett, K. Kavukcuoglu, M. Ranzato, and Y. LeCun, "What is the best multi-stage architecture for object recognition?" in *Computer Vision, 2009 IEEE 12th International Conference on*, pp. 2146–2153, Sept 2009.
- [10] Q. Ke and Y. Li, "Is rotation a nuisance in shape recognition?" in *Computer Vision and Pattern Recognition (CVPR), 2014 IEEE Conference on*, pp. 4146–4153, June 2014.
- [11] N. Srivastava, G. Hinton, A. Krizhevsky, I. Sutskever, and R. Salakhutdinov, "Dropout: A simple way to prevent neural networks from overfitting," *Journal of Machine Learning Research*, vol. 15, pp. 1929–1958, 2014.
- [12] I. J. Goodfellow, D. Warde-Farley, P. Lamblin, V. Dumoulin, M. Mirza, R. Pascanu, J. Bergstra, F. Bastien, and Y. Bengio, "Pylearn2: a machine learning research library," *arXiv preprint arXiv:1308.4214*, 2013.

- [13] J. Bergstra and Y. Bengio, "Random search for hyper-parameter optimization," *J. Mach. Learn. Res.*, vol. 13, pp. 281–305, Feb. 2012.
- [14] J. Donahue, Y. Jia, O. Vinyals, J. Hoffman, N. Zhang, E. Tzeng, and T. Darrell, "Decaf: A deep convolutional activation feature for generic visual recognition," arXiv preprint arXiv:1310.1531, 2013.
- [15] Arevalo, J., F. A. Gonzalez, Ramos-Poll'an, R., Oliveira, J. L., Lopez, M. A. G.: Representation learning for mammography mass lesion classification with convolutional neural networks. *Comp. Methods and Prog. in Biomedicine*, vol. 127, pp.248- 257, 2016.
- [16] Bishop, C. M., *Neural Networks for Pattern Recognition*: Oxford University Press, Inc., 1995.
- [17] Heaton, J., "Programming Neural Networks with Encog 2 in Java," ed: Heaton Research, Inc., 2010.
- [18] Daugman JG (1985) Uncertainty relation for resolution in space, spatial-frequency, and orientation optimized by two-dimensional visual cortical filters. *J Opt Soc Am A* 2(7):1160–1169
- [19] Foster, I, and Kesselman, C., *The Grid 2, Second Edition: Blueprint for a New Computing Infrastructure*, 2nd ed.: Elsevier, 2004.
- [20] Ramos Pollan, R., et al., "Introducing ROC curves as error measure functions. A new approach to train ANN-based biomedical data classifiers," In: 15th Iberoamerican Congress on Pattern Recognition, Sao Paulo, Brasil, 2010.
- [21] Fawcett, T., An introduction to ROC analysis. *Pattern Recognit. Lett.* 27:861–874, 2006.
- [22] Kim, J.-H., Estimating classification error rate: Repeated cross-validation, repeated hold-out and bootstrap. *Comput. Stat. Data Anal.* 53:3735–3745, 2009.
- [23] Efron, B., and Gong, G., A Leisurely Look at the Bootstrap, the Jackknife, and Cross-Validation. *Am. Stat.* 37:36–48, 1983.
- [24] Efron, B., Estimating the error rate of a prediction rule: Improvement on cross-validation. *J. Am. Stat. Assoc.* 78:316– 331, 1983.
- [25] Oliveira JEE, Gueld MO, Araújo AA, Ott B, Deserno TM (2008) Towards a standard reference database for computer-aided mammography. In: Proceedings SPIE 6915, medical imaging 2008: computer-aided diagnosis, 69151Y, pp 1Y1–1Y9. doi:10.1117/12. 770325
- [26] Gonzalez RC, Woods RE, Eddins SL (2004) *Digital image processing*. Prentice Hall, New Jersey
- [27] Sheshadri HS, Kandaswamy A (2007) Experimental investigation on breast tissue classification based on statistical feature extraction of mammograms. *Comput Med Imaging Graph* 31(1):46–48. doi:10.1016/j.compmedimag.2006.09.015
- [28] Kinoshita S, Azevedo-Marques P, Pereira R Jr, Rodrigues J, Rangayyan R (2007) Content-based retrieval of mammograms using visual features related to breast density patterns. *J Digit Imaging* 20(2):172–190. doi:10.1007/s10278-007-9004-0
- [29] Hu MK (1962) Visual-pattern recognition by moment invariants. *Ire T Inform Theor* 8(2):179–187
- [30] Teague MR (1980) Image-analysis via the general-theory of moments. *J Opt Soc Am* 70(8):920–930